Luminescence and structural properties of europium doped titania in the 600–750 °C range

Sandrine Duluard, Etienne Copin, Florence Ansart, Yannick Le Maoult, Thierry Sentenac, Philippe Brevet, Nicolas Alonso

Open Ceramics 14 (2023) 100362

Contents lists available at ScienceDirect

Open Ceramics

journal homepage: www.sciencedirect.com/journal/open-ceramics

Luminescence and structural properties of europium doped titania in the 600–750 °C range

Nicolas Alonso [a,b,c,*], Étienne Copin [c], Florence Ansart [b], Yannick Le Maoult [c], Thierry Sentenac [c], Philippe Brevet [a], Sandrine Duluard [b]

[a] Technical Department, Safran Helicopter Engines, 64511, Bordes Cedex, France
[b] Université Toulouse III – Paul Sabatier, INP, CNRS, CIRIMAT, France
[c] Clément Ader (ICA), Université de Toulouse, CNRS, IMT Mines Albi, INSA, ISAE-SUPAERO, UPS, Campus Jarlard, F-81013, Albi, France

ARTICLE INFO

Handling Editor: Dr Catherine Elissalde

Keywords:
Photoluminescence
Thermal sensor
TiO_2
Sol-gel process
Raman spectroscopy
Structural modifications

ABSTRACT

In this study, europium doped titania nanophosphors are synthetized and characterize in order to understand the relationship between structural changes induced by heat treatments and luminescence properties. After heat treatments, phase changes are observed between 600 °C and 700 °C and characterized using X-ray diffraction and Raman spectroscopy. These phase changes include the anatase – rutile transition and the apparition of secondary phases such as europium oxide and pyrochlore phase ($Eu_2Ti_2O_7$). Along with the phase changes and crystallite size evolution, the luminescence intensity of the $^5D_0 \rightarrow {}^7F_2$ transition and the lifetime decay are measured after green laser excitation (532 nm). The europium concentration is a key parameter to obtain a monotone and bijective relationship between the temperature and the luminescence behavior.

1. Introduction

Luminescent materials, and in particular, materials doped with rare earth ions have gained significant interest in the field of nanoparticles based materials [[1–3]], with the main luminescent doped materials being used in photonics devices such as: lasers [[4]], biomedical [[5]] electrochemical cells [[6]] or even displays [[7,8]]. Amongst them, titanium dioxide (TiO_2) doped lanthanides systems and the anatase phase have been widely studied because of their higher photocatalytic activity [[9]].

TiO_2 has three main polymorphs [[10]]: anatase, rutile and brookite. Only two of them (anatase and rutile) can be obtained via synthesis routes at atmospheric pressure and in the temperature range between 0 and 1200 °C. The tetragonal rutile ($P4_2/mnm$) phase is thermodynamically more stable than the anatase one ($I4_1/amd$) excepted for crystallites size below 14 nm [11], and thus, the anatase phase is favored at low temperature even by considering the thermodynamically stability of rutile phase. In any event, the irreversible anatase-rutile transformation (ART), depends significantly on the synthesis parameters (final properties of the material formed) and not only the Gibbs free energy of each phase. A typical way to achieve the stability of anatase phase over a larger range of temperature is to incorporate rare earths elements [[12]], which can shift the anatase – rutile transformation to higher temperatures.

Hishita and al [[13]]. studied the doping effect of rare earth elements on the ART. Each sample was obtained by dissolving rare earth oxides and anatase (commercial powder) with nitric acid and subsequently, heated at 500 °C during 5 h in air. Results indicate the benefit of rare earth elements to slow down the ART until 950 °C by modifying the kinetic of transformation. As example, the activation energy for pure anatase is estimated at 124 ± 3 kcal/mol vs 138 ± 4 kcal/mol for TiO_2 doped at 1 at. % of dysprosium. On another side, Setiawati and al [[12]]. focused their works on the temperature of ART for sampled of TiO_2 doped samarium and europium. A shift of 100 °C for the ART is observed with the introduction of 0.1 at. % of europium or samarium compared to pure TiO_2. However, none of these studies seems to investigate higher doping concentrations, as well as the better doping concentration for a typical doping element.

The introduction of some rare earth elements such as lanthanide ions as Eu^{3+} develops TiO_2 photoluminescence properties in the visible

* Corresponding author. 31062, Toulouse, France.
E-mail addresses: nicolas.alonso2@safrangroup.com (N. Alonso), etienne.copin@mines-albi.fr (É. Copin), florence.ansart@univ-tlse3.fr (F. Ansart), yannick.lemaoult@mines-albi.fr (Y. Le Maoult), thierry.sentenac@mines-albi.fr (T. Sentenac), philippe.brevet@safrangroup.com (P. Brevet), sandrine.duluard@univ-tlse3.fr (S. Duluard).

https://doi.org/10.1016/j.oceram.2023.100362
Received 21 February 2023; Received in revised form 17 April 2023; Accepted 26 April 2023
Available online 4 May 2023

range. The photoluminescence emission of trivalent lanthanide ions is characterized by fixed emission lines that are almost independent of the host matrix. Nevertheless, the emission intensity may vary with the host and relates the local crystallographic environment of lanthanides ions leading to the understanding of the structural environment of titanium dioxide associated with the different emission intensity of lanthanide transitions and thus, act as a probe. Antìc and al [[14]]. used the luminescence analysis to understand behavior of europium and samarium ions in the crystal lattice of TiO_2. Also, associated to the luminescence analyses, X-ray diffraction is commonly used to investigate the structural state of titanium dioxide [[15–17]]. Nevertheless, quantitative and qualitative Raman spectroscopy is not used with luminescence and X-ray diffraction, to achieve a better understanding of the stability of titanium dioxide related to the behavior of europium ions.

This paper aims to provide a better understanding of the influence of Eu^{3+} concentration (contents of 1, 3, 5 or 10 at. %) on the thermal stability of titanium dioxide and the luminescence behavior of Eu^{3+}-doped TiO_2 synthesized by a sol-gel route after short duration heat treatments in the range 600°C–750 °C. X-ray diffraction is firstly used to establish the main phases available and to estimate the crystallite sizes (Williamson and Hall method). Beside X-ray diffraction, structural analyses are made with Raman spectroscopy to push the investigation of different phases further. As said before, the local environment of rare earth ions leads to a modification of luminescence spectra, which requires a more sensitive structural technique than XRD.

Different samples with various europium concentrations are synthesized by sol-gel route, heat treated at a low temperature to eliminate the organic compounds and heat treated at 600–700 and 750 °C. Phases are analyzed with XRD and Raman spectroscopy before being compared to luminescence properties (intensity and lifetime) to correlate structural and luminescence properties.

This paper is organized as follows. In section 2, synthesis and experimental setup used for our work is presented. In section 3 the experimental results are given, followed up by a discussion about the relationship between structural modifications and luminescence properties (intensity and lifetime).

2. Experimental procedures

2.1. Precursors/materials

Titanium (IV) isopropoxide (Sigma-Aldrich, $Ti[OCH(CH_3)_2]_4$, ≥97%), europium (III) nitrate pentahydrate (Sigma-Aldrich, $Eu(NO_3)_3 \cdot 5H_2O$, 99,9% trace metals basis, isopropanol (Sigma-Aldrich, $(CH_3)_2CHOH$, ACS reagent ≥99,5%), acetic acid (Aldrich, CH_3CO_2H, glacial ACS reagent ≥99,7%) and acetylacetone (Sigma-Aldrich, $CH_3COCH_2COCH_3$, ReagentPlus ≥99%) were used as starting materials.

2.2. TiO_2: Eu^{3+} nanoparticles synthesis

Nanoparticles of Eu^{3+}-doped TiO_2 at various Eu^{3+} concentrations (1, 3, 5 and 10 at %) were prepared according to a sol-gel route adapted from Palomino-Merino and al. [[18]]. A quantity of 0.098 mol of titanium isopropoxide was mixed with 2.2 mol of acetic acid, 2.2 mol of isopropanol, 0.02 mol of acetylacetone and a stoichiometric amount of europium nitrate. The introduction of the different reagents into the mixture is presented in the flow chart in Fig. 1. The molar ratio of $[H_2O]/[Ti[OCH(CH_3)_2]_4]$ was kept equal to 1 to control the hydrolysis of titanium (IV) isopropoxide. After 15 min, the resulting TiO_2:Eu^{3+} sols were dried at 60 °C for 3 days to obtain bright titanium dioxide xerogels.

Finally, xerogels were grinded manually and the resulting powders were heat treated in order to get TiO_2:Eu^{3+} nanoparticles free from organic compounds (quantity of organic compounds <3 wt %). In order to confirm the quantity of europium in each sample, energy dispersive X-ray (EDX) was performed before the final heat treatment and results are given in Table 1.

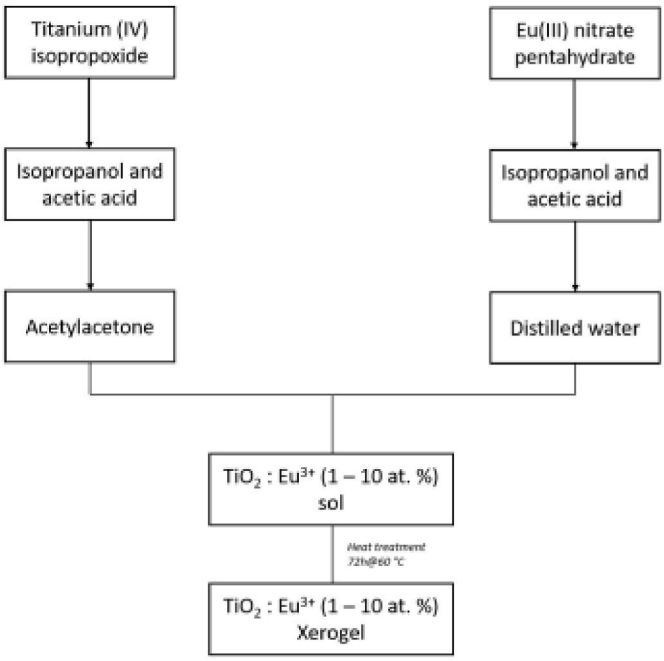

Fig. 1. Process flow chart for the preparation of TiO_2: Eu^{3+} synthetized by a sol-gel method.

An additional heat treatment (duration <20 min) at a temperature of 600, 700 or 750 °C was applied to investigate structural changes induced by heat treatments, as well as their impact on the luminescence emissions.

2.3. Characterizations

The crystalline structure and crystallite size (Williamson and Hall's equation) were analyzed by X-ray diffraction at room temperature using a RX D4 -BRUKER – AXS powder X-ray diffractometer (XRD) with Cu Kα radiation (λ = 1.5418 Å), over the range from 10 to 100° at a speed of 0.015°/min at. The phases were identified by comparison with diffraction patterns from the reference card of the JCPDS powder diffraction file.

To complete the phase analysis, Raman spectra were obtained using a confocal microscope RAMAN Labram HR 800 Yvon Jobin with an excitation wavelength of 633 nm. All spectra were collected in the range of 150–1100 cm^{-1} with a resolution of 1328 cm^{-1} at room temperature and obtained with an integration time of 60s. Raman spectroscopy was chosen because of its higher sensitivity than XRD to the presence of small amounts of the different phases such as rutile (TiO_2), anatase (TiO_2) and pyrochlore ($Eu_2Ti_2O_7$). Also, Raman spectroscopy was

Table 1
EDX analysis of europium doped samples (1, 3, 5 and 10 at. %) heat treated.

Sample	Elements			
	at. %		wt. %	
	Ti	Eu	Ti	Eu
TiO_2: Eu^{3+} (1 at. %)	98.9	1.1	96.59	3.41
TiO_2: Eu^{3+} (3 at. %)	97.06	2.94	91.23	8.77
TiO_2: Eu^{3+} (5 at. %)	94.85	5.15	14.68	85.32
TiO_2: Eu^{3+} (10 at. %)	89.95	10.05	73.9	26.1

chosen for the quantification of the anatase phase (TiO_2) [[19]], the main phase of TiO_2 typically obtained after synthesis at low temperature (<550–1000 °C). A well-known sample of crystallized anatase (assumed 100% anatase) was analyzed by Raman spectroscopy in the same conditions as the other samples, and the band area and band height corresponding to anatase lines were measured. Those values were then compared with the values obtained with the samples studied to quantify the amount of anatase phase in samples.

The luminescence emission characterization (emission spectra measurements and lifetime decays) was carried out using the excitation of a frequency-doubled, continuous wave diode-pumped Nd:YAG laser, irradiating at 532 nm (CNI Laser). For lifetime analysis, an acousto-optic modulator (1250C-974(M), Isomet) combined with a diaphragm was used to pulse the laser (laser pulses were about 20 μs). Emission intensity spectra in the 400–700 nm range were collected with a USB 2000 + spectrometer (Ocean Optics, spectral resolution of 0.15 nm) equipped with an optical fiber which collecting lens was located 20 cm above the sample surface. A high pass filter with a cut-off wavelength of 535 nm was used to filter out laser emissions. For decay time measurement, the fluorescence decay of the emission line at 610 nm was measured using a photomultiplier module (H11901-20, Hamamatsu) equipped an optical fiber. The optical fiber is associated with a lens, located 20 cm above the sample surface and a narrow band filter is used to be centered on the 610 nm emission of Eu^{3+} (610 nm, FWHM: 10 nm). In addition to the high pass filter with a cut-off wavelength of 535 nm, a notch filter at 532 nm was used to filter out laser emissions. All measurements were carried out at room temperature.

3. Results

3.1. Structural analysis

TiO_2:Eu^{3+} nanopowders structural properties were analyzed by X-ray diffraction and Raman spectroscopy, Fig. 2 (a)-(d) illustrate the XRD patterns of synthesized TiO_2:Eu^{3+} at doping concentrations of 1 at. %, 3 at. %, 5 at. % and 10 at. % and without europium, Fig. 2 (e). After heat treatment at 600 °C, all samples only exhibit diffraction peaks corresponding to the metastable phase anatase (JCPDS 021–1272). However, the crystallization state appears to be much less advanced for 5 at. % and 10 at. % samples which exhibit large and weak diffraction peaks (Fig. 2 (c) and (d) respectively) as compared to the more intense and better-defined diffraction peaks in 1 at. %, 3 at. % and un-doped samples diffraction patterns (Fig. 2 (a), (b) and (e) respectively).

After a treatment at 700 °C, no significant changes are observed in the europium doped TiO_2 patterns other than a slight intensity increase of diffraction lines for the poorly crystallized samples at 5 at. % and 10 at. % dopant concentration compared to the un-doped titania which already exhibits the rutile phase (JCPDS 021–1276). After a treatment at 750 °C, samples at 1 at. % and 5 at. % exhibit diffraction lines characteristic of the rutile phase (much more pronounced at 1 at. %) in

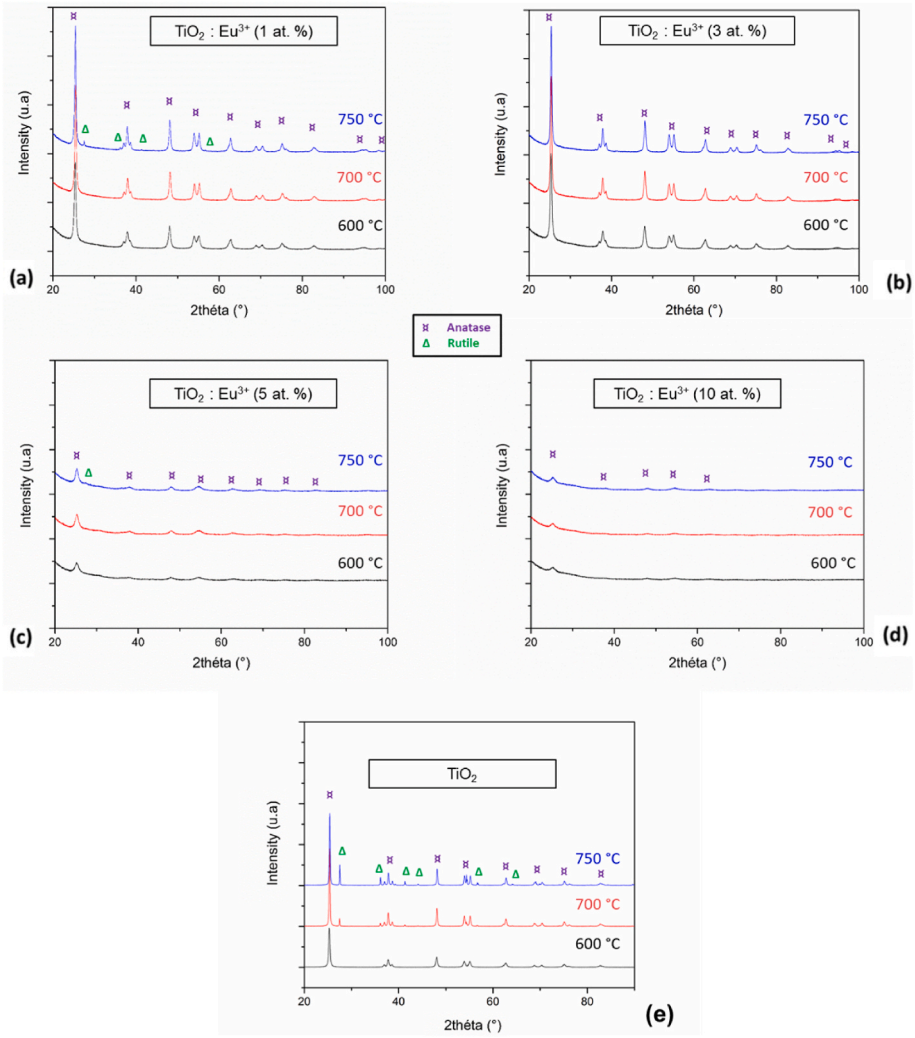

Fig. 2. XRD patterns of TiO_2:Eu^{3+} samples doped at 1 at. % (a), 3 at. % (b), 5 at. % (c), 10 at. % (d) and un-doped TiO_2 (e) heat treated at different temperatures.

addition to anatase (Fig. 2 (a) and (c) respectively), while only anatase peaks remain present for 3 at. % and 10 at. %. It should also be noted that, the advancement of the crystallization of the anatase phase remains lower for high dopant concentration (5 at. % and 10 at. %) than un-doped TiO_2 or TiO_2 doped at (1 at. % and 3 at. %) samples.

The evolution of anatase crystallite size with heat treatment temperature, determined from the diffraction patterns, is given in Fig. 3 for all samples. Anatase crystallite size increases with heat treatment temperature for all dopant contents, but decreases with Eu^{3+} concentration at any given temperature studied: from 600 °C to 750 °C, the anatase crystallite size increases from 33 nm to 66 nm for titania sample (+100%), from 24 nm to 35 nm at 1 at. % (+46%), from 21 nm to 24 nm at 3 at. % (+13%), from 9 nm to 14 nm at 5 at. % (+56%), and from 6 to 11 nm at 10 at. % (+83%). The trend is thus similar for all concentrations with the exception of the 3 at. % doped sample for which the rate of crystallite size increase with temperature appears to be lower than for the rest of the samples (+13%). It is noteworthy that, in all cases, europium doped titanium dioxide samples have a lower increase of the crystallites size than the pure titania sample.

To sum it up, the material exhibits the anatase (JCPDS 021–1272) crystalline structure of TiO_2 for each sample with a major difference in the crystallization state which is less advanced at (c) 5 and (d) 10 at. % of Eu^{3+} compared to (a) 1, (b) 3 at. % and un-doped titania (e). Additional structural analyses (Raman spectroscopy) were performed to confirm these results and are presented later in this paper.

Raman spectra of TiO_2:Eu^{3+} powders treated in the 600–750 °C range are displayed in Fig. 4. The characteristic phonon bands with six active modes associated to anatase according to factor group theory are found and confirm the presence of anatase phase in all the studied samples for temperatures between 600 and 750 °C (the three bands at 144, 197 and 640 cm^{-1} assigned to the E_g mode, the band at 399 cm^{-1} B_{1g} mode and the band at 516 cm^{-1} which is assumed to be the sum of the two A_{1g} and B_{1g} modes bands expected at 514 and 519 cm^{-1} [[20]]). Raman active fundamentals band of the ordered rutile structure at 143, 447, 612 and 826 cm^{-1} corresponding to B_{1g}, E_g, A_{1g} and B_{2g} are researched but none of them seem to be present in the samples, exepted for the un-doped titania between 600 and 700 °C (Fig. 4 (e)) or at 5 at. % between 700 and 750 °C (Fig. 4 (c)). The 143 cm^{-1} band of rutile being coincident with the 144 cm^{-1} of anatase, it is indeed not possible to conclude on the presence of ordered rutile in the absence of the other bands but, further analysis (not shown here) has been made with higher integration time to investigate the presence of rutile phase and it was not detected.

Nevertheless, an unexpected band at about 235 cm^{-1} is found for samples doped at 1 at. %, 5 at. % and 10 at. % (Fig. 4 (a), (c) and (d)), which could correspond to a disordered rutile lattice. Hara and Nicol [[21]] proposed that this band is induced by the disordered rutile lattice and should decrease with increasing ordering in the rutile lattice. The presence of disordered rutile is observed from 600 °C in the 10 at. % sample, and from 700 °C in the 1 at. % and 5 at. % samples. Both ordered and disordered rutile seem to coexist in the 5 at. % sample at 700 °C and 750 °C. None of the rutile phases is detected in the 3 at. %-doped sample, even with a higher integration time (t < 120s).

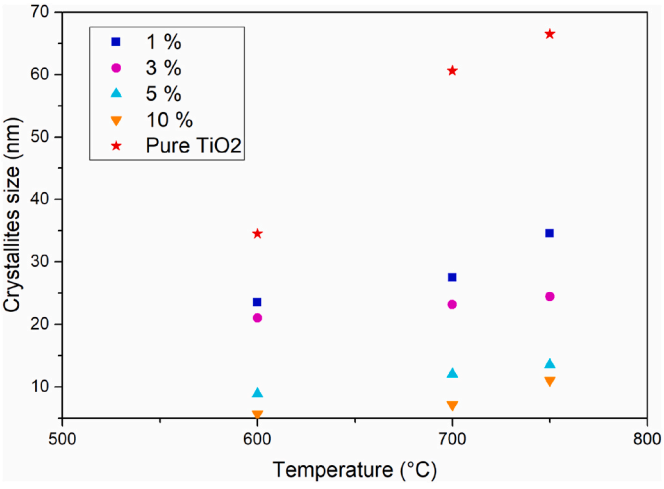

Fig. 3. Evolution of TiO_2 anatase crystallites size with heat treatment for different doping concentrations.

Those results differ from the XRD analysis because of the greater sensitivy of Raman spectroscopy. The rutile diffraction peaks were observed only after treatment at 750 °C for samples doped at 1 at. % and 5 at. %, suggesting that the volume fractions of rutile involved are small. Hence, rutile phase (disordered) is detected at lower temperatures (600 °C for 10 at. % and 700 °C for 1 and 5 at. % europium doped titanium dioxide) than by XRD. In addition, only the un-doped sample, which is by far the less complex compound analyzed, shows strong similitude between XRD (Fig. 2 (e)) and Raman (Fig. 4 (e)) analysis.

In addition to anatase and rutile phases, Raman spectra of some samples exhibit two other bands centered at 320 and 350 cm^{-1}. The first additional band corresponds to the presence of pyrochlore $Eu_2Ti_2O_7$ phase [[22]], it is found at 750 °C in 1 at. %-doped sample (Fig. 4-a), and at a lower temperature of 700 °C and 600 °C respectively for the 5 at. %-doped and 10 at. %-doped samples (Fig. 4-c and Fig. 4-d). The intensity of this band increases with increasing heat treatment temperature for a given Eu^{3+} concentration, or when increasing europium concentration at a given firing temperature. One exception is the 3 at. %-doped sample for which no pyrochlore phase is detected.

The second additional band at 350 cm^{-1} indicates the presence of europium in its oxide form (Eu_2O_3) [[23]]. It is found that samples heat treated from 600 °C to 750 °C for 1 and 10 at. % and only at 600 °C for 5 at. %, but none is detected for a concentration of 3 at. % of europium. The existence of europium oxide could be explained by the utilization of europium nitrates as precursors, which thermal decomposition product is europium oxide above 300 °C [[24]]. Hence, it is assumed that part of the europium nitrates could be transformed into oxides before being integrated into the crystal lattice of TiO_2.

Fig. 5 shows the evolution of the surface area of Raman spectra bands corresponding to each phase as a function of temperature for each dopant concentration, as attempt to make a quantitative estimation of the phase composition change with concentration. The sample doped at 3 at. % stands out by being the only sample made of a single phase, anatase, at all investigated temperatures. In the first place, the pure TiO_2 sample is composed of anatase phase, which increases gradually until 700 °C and decreases afterward; contrary to ordered rutile (detected at least at 700 °C), increasing from 700 °C to 750 °C. TiO_2:Eu^{3+} doped at 1 at. % at 600 °C initially contains anatase as well as small amounts of europium oxide and disordered rutile phases (not enough to be detected by XRD). The amount of the two latter seems to increase after treatment at 700 °C and 750 °C (rutile diffraction peaks appear in the diffraction pattern), and at 750 °C some amount of pyrochlore appears, yet too low to be detected by XRD. The sample doped at 5 at. %, as the one doped at 1 at. %, also contains small amount of Eu_20_3 and disordered rutile at 600 °C, and exhibits also an increase of disordered rutile between 600 °C and 750 °C and the apparition of pyrochlore phase at 750 °C. The main difference lays in the apparition of ordered rutile between 700 °C and 750 °C in the XRD. At last, the 10 at. % doped TiO_2 exhibits the presence of the pyrochlore phase at the lowest temperature i.e. 600 °C along with anatase, europium oxide and disordered rutile. Hence, increasing the concentration of europium is likely to destabilize anatase lattice by promoting transformation and apparition of different phases, excepted for the particular concentration of 3 at. % which seems to be stable until 750 °C at least.

Finally, Fig. 6 shows the evolution of the quantity of anatase, the major phase within samples, with temperature and Eu^{3+} concentration. It was evaluated by comparing samples with a well-known commercial

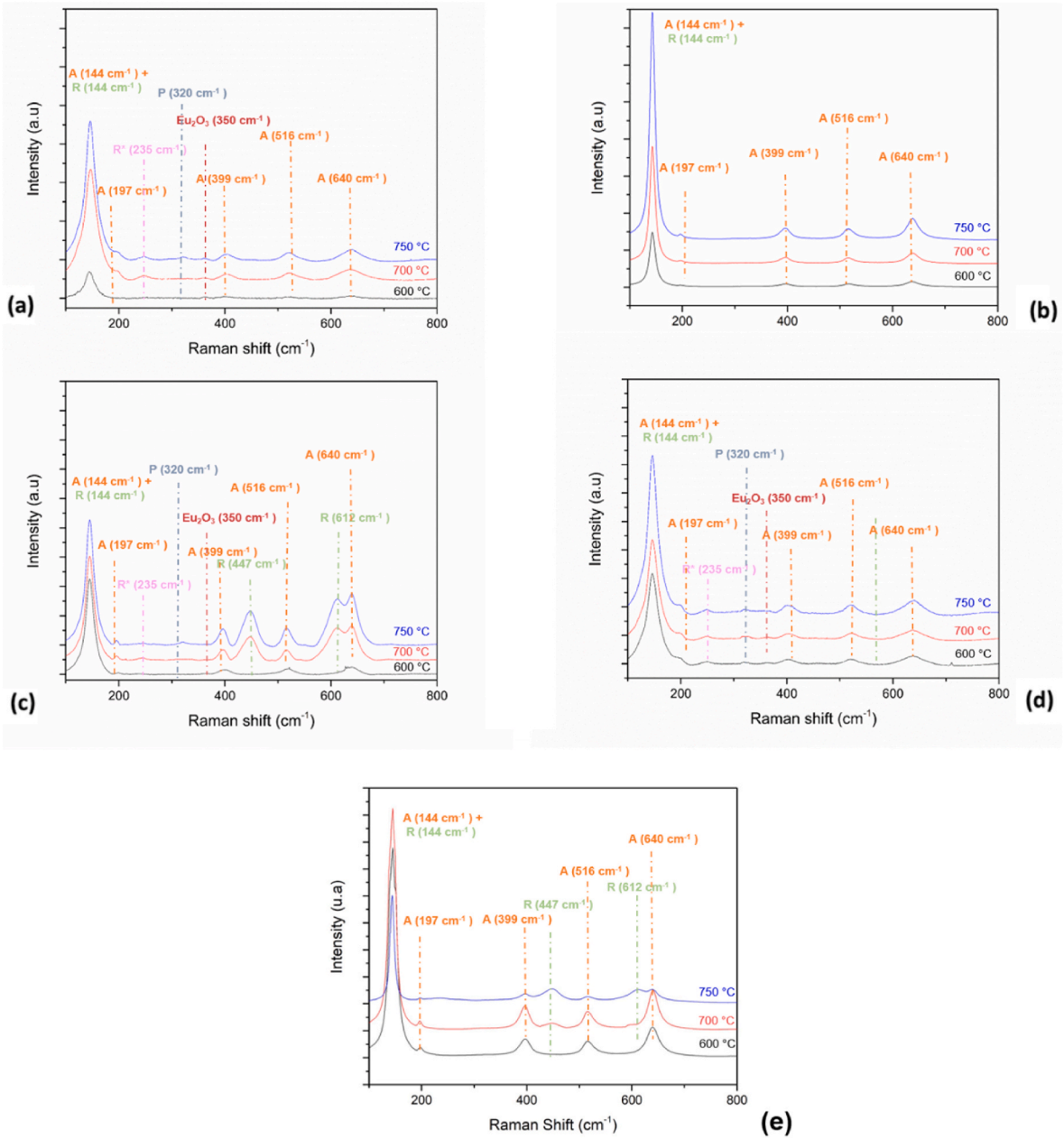

Fig. 4. Raman spectra of TiO_2:Eu^{3+} samples doped at 1 at. % (a), 3 at. % (b), 5 at. % (c), 10 at. % (d) and un-doped TiO_2 (e), fired at different temperatures. A: anatase, R: rutile (ordered), R*: rutile (disordered), P: pyrochlore $Eu_2Ti_2O_7$ and Eu_2O_3 for europium oxide.

powder of pure anatase (Sigma Aldrich, 100% anatase). It should be noted that this method only gives the amount of anatase, the remaining is assumed being non fully crystallized material (for most part) and/or the other phases observed (Eu_2O_3, disordered rutile, pyrochlore $Eu_2Ti_2O_7$). Unsurprisingly given the XRD patterns obtained, the 10 at. % doped sample contains the lowest quantity of anatase at 600 °C (2.2%), which does not increase much with treatment temperature (3.2% at 750 °C), while the un-doped sample, contains the highest quantity of anatase phase on the thermal range studied (69% at 600 °C, 92% at 700 °C and 78% at 750 °C). Interestingly, the doped sample containing the highest fraction of anatase is the sample doped at 3 at. % (60.6% at 600 °C increasing to 71.6% at 750 °C), not the sample with the lowest Eu^{3+} content (30.4% at 600 °C, increasing to 45.8% at 750 °C for 1 at. %). For the sample with 3 at. % of Eu^{3+} as no other phase was detected, the remaining fraction is assumed to be amorphous material (39.4 at 600 °C vs 28.4% at 750 °C), which fraction decreases with treatment temperature. At 1 at. %, the content of anatase is significantly lower but shows a trend to increase with temperature (30.4% at 600 °C and 45.8% at 750 °C). At 5 at. % Eu^{3+}, the quantity of anatase is as low as in the 10 at. % at 600 °C (4.0% for 5 at. % and 2.2% for 10 at. %), but is greatly enhanced by treatments at 700 °C and 750 °C to reach levels very closed to that achieved with 1 at. % doping (31.2% at 700 °C and 42.0% at 750 °C). Surprisingly, the sample with a unique phase (anatase) has the lowest kinetic increase on the thermal range studied (+20% of the initial %); in comparison samples doped at 1, 5 and 10 at. % have an increase of anatase phase by around +50%, +955% and +50% respectively.

Therefore, TiO_2: Eu^{3+} 1–10 at. % appears to be a rather complex system constituted of various potential phases, in contrast to the un-doped compound, which composition and proportion are very sensitive to Eu^{3+} concentration and to the short heat treatment temperature in the range 600°C–750 °C, although it seems to exist a domain of stability for a single anatase phase of TiO_2 around 3 at. % doping of Eu^{3+}.

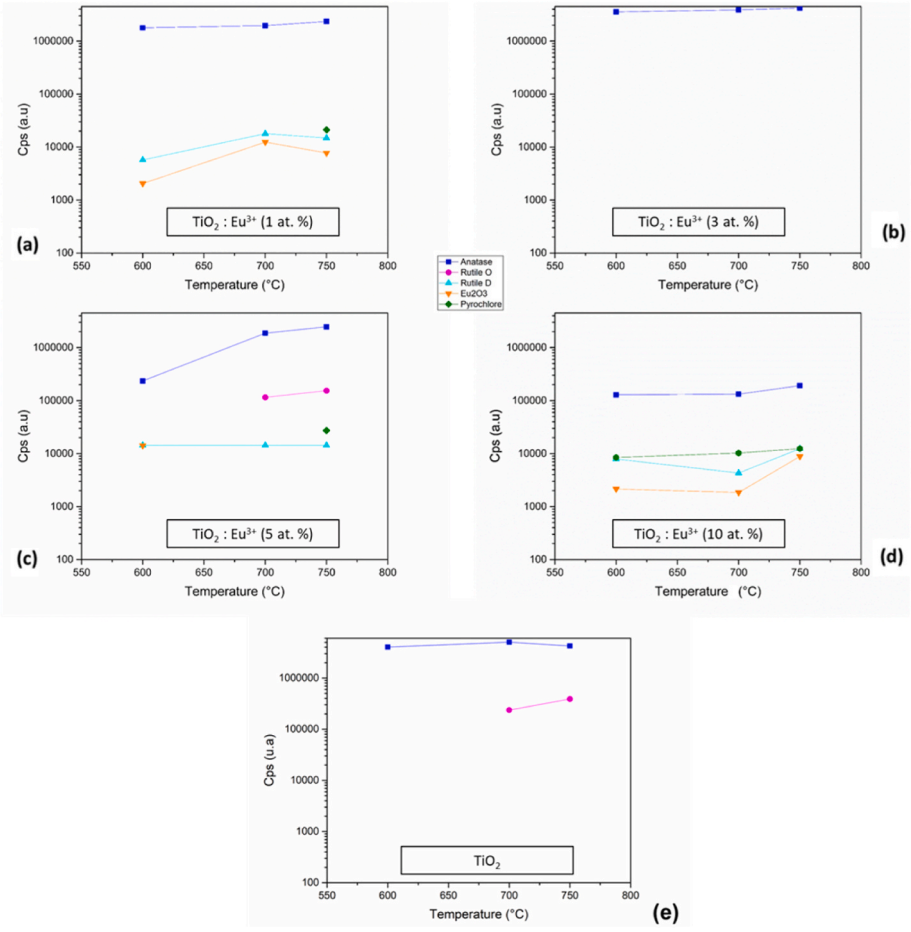

Fig. 5. Integrated peaks areas of different phases detected in Raman spectra, as a function of temperature for TiO_2 with 1 at. % (a), 3 at. % (b) 5 at. % (c), 10 at. % (d) of Eu^{3+} and un-doped TiO_2 (e).

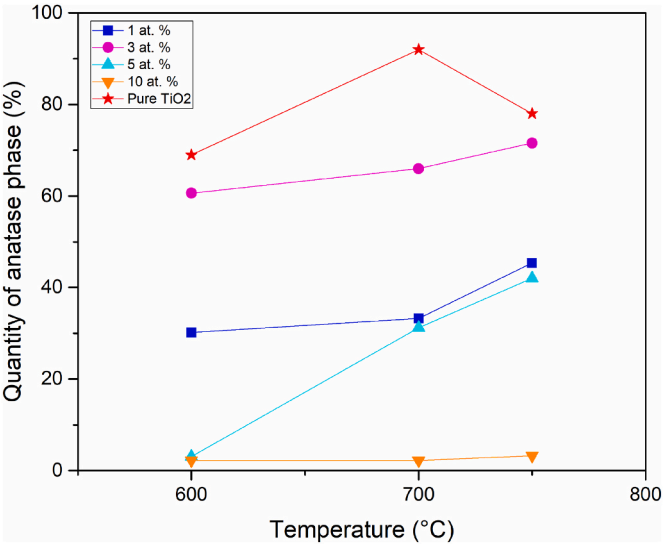

Fig. 6. Quantity of anatase phase as a function of heat treatment temperature.

Fig. 7 shows the photoluminescence emission spectra of TiO_2: Eu^{3+} powders. Upon the excitation of a 532 nm laser, samples exhibited the typical emission lines from the $^5D_0 \rightarrow {}^7F_J$ transitions (J = 0, 1, 2, 3 and 4) of Eu^{3+} ions. The bands ascribed to the f–f transitions are: $^5D_0 \rightarrow {}^7F_0$ (578 nm), $^5D_0 \rightarrow {}^7F_1$ (582–603 nm), $^5D_0 \rightarrow {}^7F_2$ (605–634 nm), $^5D_0 \rightarrow {}^7F_3$ (649–658 nm) and $^5D_0 \rightarrow {}^7F_4$ (682–712 nm) [25].

Regarding spectra analysis, all samples exhibit the $^5D_0 \rightarrow {}^7F_0$ transition at 578 nm. The occurrence of this transition is the result of the breaking of the selection rules because 0-0 transition is forbidden by the Judd-Ofelt rules. Existence of this transition suggests that europium ions occupy C_{2v} symmetry confirmed by the presence of the $^5D_0 \rightarrow {}^7F_2$ transition at 610 nm, allowed when europium ions are positioned in sites without an inversion symmetry, as the C_{2V} site symmetry [[25]]. Besides, the $^5D_0 \rightarrow {}^7F_2$ transition is often used as a structural probe, to understand the structural position of europium ions. The various morphologies of the $^5D_0 \rightarrow {}^7F_2$ transition peak for the different samples can be observed in Fig. 7-a-b-c-d, for various heat treatments. As well, shapes of the $^5D_0 \rightarrow {}^7F_2$ hypersensitive transition of 1 and 3 at. % samples ((a) and (b)) are similar whereas the samples doped at 5 and 10 at. % ((c) and (d)) have the same peak shape without peak shoulders. This major difference involves that europium ions are not located in the same lattice site, and so, the local structure is different between samples doped at 1 and 3 at. % (a and b) versus sampled doped at 5 and 10 at. % (c and d).

First of all, it can be observed on Fig. 8 that emission intensity, especially pronounced for the $^5D_0 \rightarrow {}^7F_2$ line at 613 nm, increases with heat treatment temperature between 600 °C and 750 °C for samples doped with 1 at. %, 3 at. % and 5 at. % of Eu^{3+}, although the level of increase varies. At 1 at. %, the emission increases brutally from 600 °C to 700 °C (+208%) then, it is rather limited (+4% for the emission peak at 610 nm from 700 °C to 750 °C). At 3 at. %, there is a +120% increase between 600 °C and 700 °C, followed by a more modest +15% increase between 700 °C and 750 °C. At 5 at. %, intensity increases by +160% between 600 °C and 700 °C and by +45% between 700 °C and 750 °C.

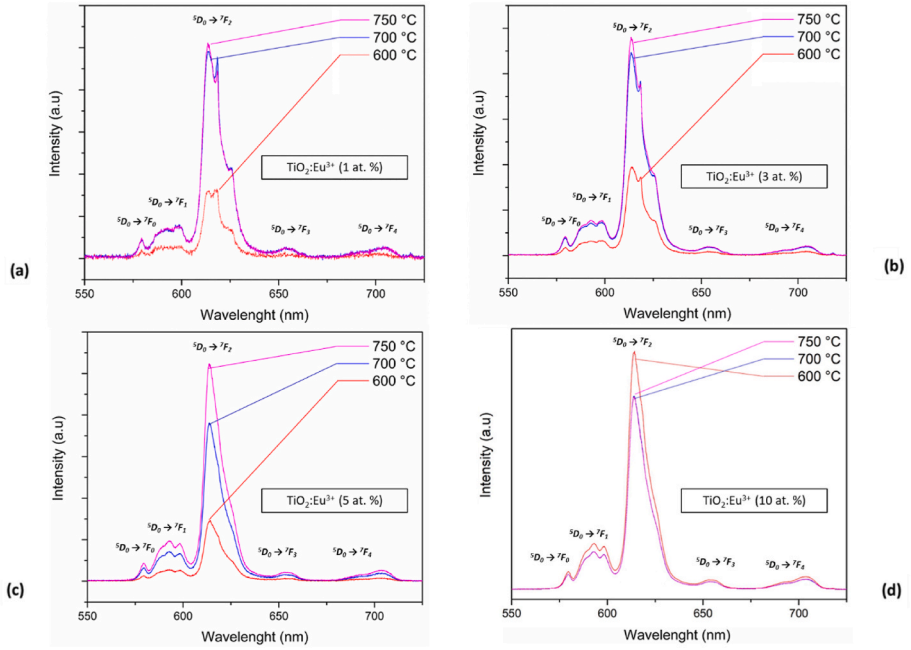

Fig. 7. Evolution of photoluminescence emission spectra with temperature for TiO_2: Eu^{3+}at (a) 1 at. % - (b) 3 at. % - (c) 5 at. % and (d) 10 at. %.

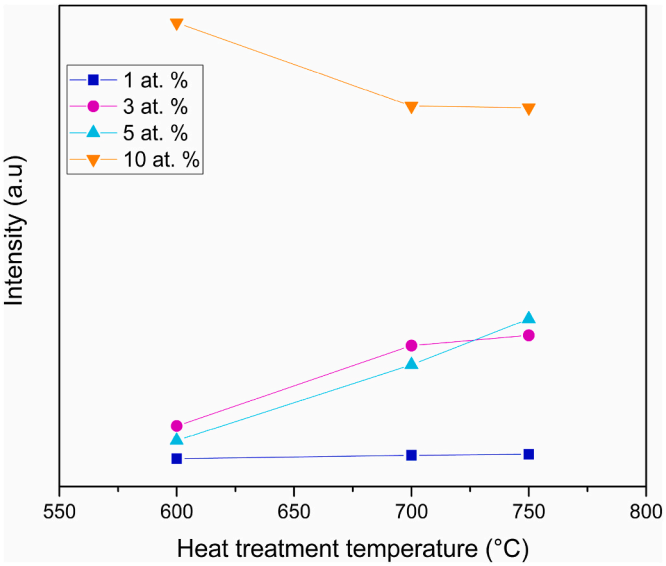

Fig. 8. Luminescence intensity as a function of temperature for 1–10 at. % of europium ions.

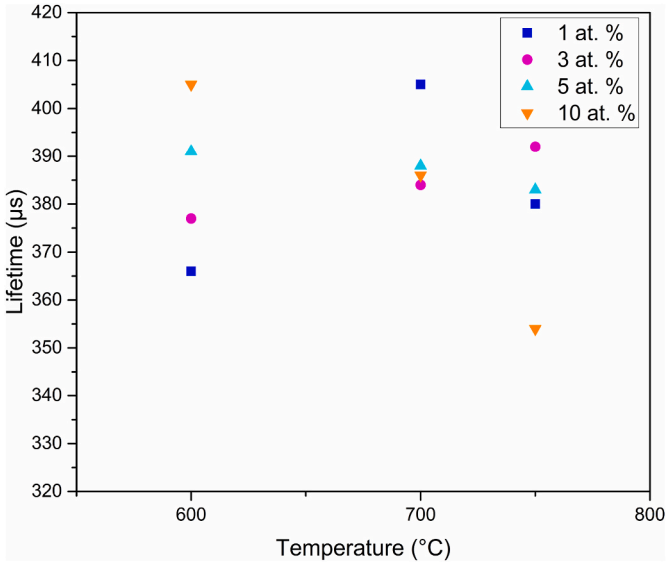

Fig. 9. Photoluminescence lifetime of the $_5D^0 \rightarrow {}_7F$ [2] emission at 610 nm as a function of heat treatments for different europium concentrations in TiO_2.

The sample doped at 10 at. % shows an opposite trend, the intensity is the highest at 600 °C, and presents a decreasing trend (−15%) up to 750 °C.

The evolution of the photoluminescence lifetime of the $^5D_0 \rightarrow {}^7F_2$ transition at 610 nm with heat treatment temperature for all samples is displayed in Fig. 9.

At the lowest doping concentration (1 at. %), the lifetime has a non-monotonic evolution (increase from τ = 366 μs at 600 °C to τ = 406 μs at 700 °C (+10%), then decreases to τ = 380 μs at 750 °C (- 4%)). The sample doped at 3 at. % exhibits only a monotonic increase with heat treatment temperature, with a measured lifetime of 377 μs at 600 °C and 393 μs at 750 °C (+5%). Finally, for higher concentrations (5 and 10 at. %), the lifetime decreases between 600 °C and 750 °C from 392 μs to 383 μs (−2.5%) and 405 μs–354 μs (−13%) respectively. Lifetimes found in this study are comparable to these discussed by Antic and al [[14]]. which use a similar synthesis method with τ = 460–680 μs, as compared to τ = 354–406 μs for our nanophosphors.

3.2. *Discussion: effect of crystallization and phase change on the luminescence mechanism*

3.2.1. *Anatase phase formation and its thermal stability*

Titanium dioxide is found in three main polymorphs, anatase, rutile and brookite. At atmospheric pressure, the anatase might form first, followed by an irreversible phase transformation to rutile phase around 600 °C [[26]]. In un-doped titanium dioxide, the anatase-rutile-transformation (ART) begins, as expected, somewhere between 600 and 700 °C, contrary to doped titanium dioxide in which, depending on the dopant, the dopant might stabilize one of the two phases or act as a catalyzer of the ART. In addition, the increase of

doping concentration may decrease the crystallization kinetic due to lattice distortion produced by doping ions. Generally speaking, cationic doping works as a stabilizer if the ionic radius (r > 75 p.m.) or the valence (x > 4) are higher than those of Ti^{4+} atoms, while it may promote rutile or other phases if the ionic radius (r < 75 p.m.) or valence are lower than those of Ti^{4+} atoms. Hanaor and Sorell [[26]] investigated the effect of cations, and in particular, lanthanide ions. Borlaf and al. have confirmed the stabilizing effect of europium acting as inhibitor of the anatase-rutile transformation (ART), europium ions could stabilize anatase until 955 °C [[27]] for thin films or above 765 °C [[15]] for nanoparticles synthetized by sol-gel route with 3 at. % of europium. In comparison, 1 and 2 at. % of europium ions leaded to an ART at 910 and 935 °C for thin films and 690 and 635 °C for xerogels respectively, indicating that an increase of doping concentration stabilizes anatase phase.

In the present study, at the lowest firing temperature, 600 °C, anatase is the main phase formed for all samples, and its crystallization seems to be enhanced for titanium dioxide doped at 1 and 3 at. % (anatase content >30%, Fig. 6) compared to higher concentrations (anatase content <5 % at 5 at. % and 10 at. %, Fig. 6). It is even the only phase present at 3 at. % of europium at 600 °C (Figs. 2 and 4). As explained by Zhang et al. [[28]], increasing concentration of europium leads to a shift of the onset of crystallization, yielded by europium which diffuses into titanium dioxide lattice forming an interstitial solid solution. After treatment at 700 °C, the crystallization of the sample doped at 5 at. % is finally activated (quantity of anatase close to the TiO_2: Eu^{3+} 1 at. % at the same temperature) unlike the one doped at 10 at. % for which the enhancement of the crystallization of anatase remains very low even after firing at 750 °C. This analysis suggests that a quantity of europium in the range of 3 at. % favors the crystallization of anatase (anatase content 60.6% at 3 at. % vs 30.4% at 1 at. % at 600 °C). At higher concentration ([C] ≥ 5 at. %), the anatase crystallization is impacted and shifted to higher firing temperature, and the resulting material is mostly amorphous.

Europium ions have a tendency to inhibit the growth of crystallite by forming interstitial lattice solid solutions that hinders the migration of the crystallite boundary, increasing the number of defects and therefore decreasing the kinetic of crystallite growth. It would apply drag forces on boundary movement and the grain growth (by restricting direct contact of grains) or by increasing the number of defects which could result in lower grain boundary mobility and thus, lower crystallites size (i.e. lower crystallization kinetics) [[29]] even at high temperature, as illustrated in Fig. 3 and determined using the Williamson and Hall method. In addition, oxygen vacancies, correlated with doping concentration (increasing the doping concentration leads to a higher amount of oxygen vacancies) induced by a charge imbalance (Eu^{3+}/Ti^{4+}) might affect the crystallites size. Hsu and al. reported [[30]] that oxygen vacancies induce stresses and defects and thereby reduce the long range ordering (i.e. reduce crystallites size) [[31]].

Considering these effects, it is evident that a specific concentration of europium would reasonably stabilizes the first formed phase (anatase), yielding to the promotion of this phase regardless the nature and quantity of the other phases. As described above, oxygen vacancies and induced stress might reduce the long-range ordering enough to reduce the kinetic of crystallization of all the phases and hence, being a contributing factor to the stabilization of the anatase phase. 1 at. % of europium appears to be not sufficient to support the stability of anatase phase at high temperature, formation kinetics of phases might be affected as well as the kinetic of growth of crystallites, but, not enough to ensure the full stabilization of anatase (europium oxide and disordered rutile are formed at 600 °C, at least, and pyrochlore between 700 °C and 750 °C).

If considering the inhibition effect of grain growth mentioned above, at 3 at. % lower crystallite sizes could be expected but also a lower state of crystallization of anatase phase. However, it is observed experimentally that while the crystallite sizes indeed is reduced (21 nm vs 23.5 nm for 3 and 1 at. % of europium respectively), anatase happens to be the unique phase created, in a higher quantity (60.6% vs 30.4% for 3 and 1 at. % of europium ions). Additionally, the inhibition effect of crystallite growth when heat-treated seems to be higher at 3 at. % (+13% in the 600–750 °C thermal range) because of the insertion of europium ions in interstitial sites.Experimentally, exclusively the decrease of the kinetic of crystallite growth is found and the anatase phase happens to be the unique phase created, promoting its stability and the quantity of phase formed. At concentrations of 5 at. % and higher, the stabilizing effect is not found, and, rutile, europium oxide, and pyrochlore phases are present in higher quantity. Hypothetically, the benefic effect of europium additions (i.e. reducing globally kinetics formation of phases and promoting the anatase phase) would be lost because of the difficulty of europium ions, available in too high quantity, to go into titanium dioxide lattice interstitial sites.

Moreover, europium ions can contribute to shift the ART to higher temperatures, depending on the concentration. Samples doped at 1, 5 and 10 at. % analyzed by Raman spectroscopy (Fig. 4) already exhibit disordered rutile after a heat treatment at 600 °C. Many authors who investigated the ART for nanoparticles synthesized by sol gel method, as Borlaf and al. [[15,27]], determined the ART to lay between 635 and 765 °C, respectively, for 1 and 3 at. % of europium. However, those conclusions were based on XRD analysis, in which the phase detection limit is known to be about few percent, depending of the preparation quality. Thanks to a higher sensitivity, Raman spectroscopy permit a more in-depth phase analysis. Disordered rutile is associated with the 235 cm^{-1} band by Nicol [[21]] and evocated by Balachandran and al. [[32]]. This band decreases due to increasing order and in fine, increase of rutile ordered phase. Europium ions, inhibiting the grain growth and decreasing the grain boundary mobility may leads to facilitating the formation of disordered rutile by blocking the reconstructive transformation (ART) and hence, distorting titanium dioxide lattice. At an intermediate concentration around 3 at. % of Eu^{3+}, it also appears to fully inhibit the formation of rutile and any other phase up to at least 750 °C, which represent a shift of the ART by at least 150 °C compared to the other concentrations studied.

The presence of europium or, in general, of rare earth ions, may involve the possible formation of other non-desired phases such as Eu_2O_3 (europium oxide) or $Eu_2Ti_2O_7$ (pyrochlore). The former oxide is detected at low (1 at. %) and high concentrations (5 and 10 at. %) at 600 °C (Fig. 4) and is assumed to originate from the thermal decomposition of the $Eu(NO_3)_3$ precursor used, suggesting an incomplete integration of Eu within the TiO [2] lattice for those concentration. This is expected for high dopant concentrations but not for low concentration (e.g 1 at. %) since no Eu_2O_3 oxide is detected at 3 at. % (Fig. 4). Nonetheless, only the kinetic effect of doping concentration might be discussed here since heat treatment are no longer than 20 min. Once more, this suggests the existence of a kinetically stable TiO_2:Eu^{3+} system around 3 at. % of Eu^{3+}.

The characteristic band of europium oxide (350 cm^{-1}) increases with the heat treatment temperature until its brutal vanishing for treatment at 750 °C, suggesting it is no longer stable at a temperature between 700 °C and 750 °C (Fig. 5). Its presence is not often studied or reported for TiO_2:Eu^{3+} syntheses, but again this is probably due to the use of characterization techniques less sensitive than Raman spectroscopy.

The second non-desired phase detected, $Eu_2Ti_2O_7$, is observed after a heat treatment at 750 °C for 1 and 5 at. % and already after a heat treatment at 600 °C for 10 at. % of europium. It thus appears at a far lower temperature than the ones reported in the literature for Eu^{3+} doped titanium dioxide. XRD studies by Borlaf and al [[15,27]]. reported an apparition of the pyrochlore phase for 1 at. % of europium around 950 °C and 3 at. % at 900 °C. Ninghthoujam and al [[33]]. studied the pyrochlore phase in the titanium dioxide doped with 5 and 10 at. % of europium ions, and determined its formation close to 900 °C for both sample by XRD. Again, the sensitivity of the detection methods used in those studies can explain the higher temperature onset of the

formation of $Eu_2Ti_2O_7$ as indicated in our study when XRD and Raman spectroscopy are compared.

The apparition and stability of the pyrochlore phase at low temperature (750 °C for 1 at. % and 600 for 10 at. %, Fig. 4) are likely related to the increasing difficulty for europium ions to go into titanium dioxide lattice interstitial sites as the europium concentration increases. Nevertheless, the sample doped at 3 at. % of europium ions appears to be the only one exempt of pyrochlore phase and again, the only concentration studied permitting the stability of anatase phase after heat treatments between 600 °C and 750 °C.

3.2.2. Parameters influencing the luminescence properties

3.2.2.1. Major mechanism. Usually, phosphors in an amorphous state, as it is often the case when synthesized by a sol-gel route (low to moderate heat treatment conditions), show weak and broad fluorescence emission peaks induced by the large variety of crystallographic environments seen by dopant ions in the host matrix. It can result in a wide and non-uniform distribution of energy level configuration for the population of dopant ions, leading to broader and less intense emission lines quite different from the one observed in a fully crystallized matrix. Furthermore, amorphous environment can be rich in crystal defects favoring non-radiative relaxation pathways, explaining the lower emission intensity level often observed. At last, the presence of residual organic functional groups resulting from the synthesis that acts as luminescence quenchers can further affect the luminescence emissions of the phosphor.

When heat treating such phosphors at high temperature, intensities of each transition generally increases and emission lines become sharper and better defined as a consequence of different chemico-physical phenomena, which include phase change, crystallization (annihilation of crystal defects, homogenization of the local environments, crystallite size increase), elimination of quenchers. Therefore, if the phosphor is chemically stable (no phase change), with a morphology that does not change a lot in the thermal range (samples do not undergo drastic change in specific surface), and it does not contain organic compounds (or in negligible quantity). The only remaining major mechanisms, which could be responsible of an increasing intensity in the luminescence spectrum, is likely the crystallization process (i.e. amorphous to crystalline transition and increase of crystallites size). As it is likely to be the case for the 3 at. % doped sample studied here.

3.2.2.2. Europium in TiO_2 anatase lattice. Ti^{4+} ions, in the anatase lattice, belong to the D_{2d} crystallographic point group symmetry. The Eu^{3+} ions in interstice lattice distort the lattice and lead to a decrease to a lower site symmetry (S_4, C_{2v} or D_2) as compared to TiO_2 due to the difference in ionic radius and the charge difference, which generates oxygen vacancies. Europium ions located at S_4 or D_2 sites symmetry (sites with inversion symmetry) have their electronic dipole (ED) transitions forbidden, especially the $^5D_0 \rightarrow {}^7F_2$ transition, often called "hypersensitive" due to the high sensitivity to the environment, unlike ions situated in C_{2V} sites, slightly distorted, which have their ED transitions allowed. Three crystallographic sites are described as the main sites for Eu^{3+} in doped anatase TiO_2 within the three principal sites S_4, C_{2v} or D_2. [[34–36]]. These sites could be divided into two categories:

- Site I, europium is located in a disordered environment with the lowest symmetry, near the crystal surface with a distorted lattice. Luminescence emissions are the same for all europium ions in the site I as the free trivalent europium ion.
- The second category is the position of Eu^{3+} in an ordered lattice environment (crystallization). For this option, two types of crystallographic sites are found. A site (site II) with a high degree of symmetry like D_2 (with an inversion center) and another one (site III) with a lower degree of symmetry (C_{2v}) and without inversion center.

If the number of europium in the ordered lattice is equivalent for site I and site II, the intensity might increase along with the crystallization (i.e. thermal treatment temperature for treatments of the same duration). The evolution of the integrated intensity of the $^5D_0 \rightarrow {}^7F_2$ transition with heat treatment temperature, plotted for each dopant concentration in Fig. 8, illustrates this behavior.

The sample containing 3 at. % of europium which only exhibited an increase of crystallized phase proportion (Figs. 2 and 6) and crystallite size (Fig. 3) without any phase change (Fig. 4), shows a monotonic intensity increase on the whole temperature range as well as a monotonic increase of lifetime decay. Considering its emission spectrum, (Fig. 7-b), the $^5D_0 \rightarrow {}^7F_2$ transition reveals an homogenization of the corresponding peak (i.e. homogenization of the environment of the europium population). At the lowest treatment temperature, europium ions are probably mainly located in "site I" or in an amorphous environment with a broad peak around 613 nm [37]. With increasing heat treatment temperature, the peak is getting sharper as ions are occupying in majority the same ordered site.

3.2.2.3. Influence of the secondary phases. Contrary to the 3 at. % Eu^{3+} doped sample, the lower dopant concentration sample (TiO_2: Eu^{3+} 1 at. %) does not stabilize the anatase phase and other phases are present, such as Eu_2O_3, disordered rutile or $Eu_2Ti_2O_7$ pyrochlore phase (at a higher firing temperature of 750°C, Fig. 4). One possible explanation of the very small photoluminescence intensity increase observed with heat treatments at those concentrations as compared to the 3 at. % doped (increase of 249% between 600 °C and 750 °C, Fig. 7), arises from the formation of undesired phases which consume europium without leading to the same level of photoluminescence intensity than anatase (e.g. rutile and Eu_2O_3 phases at 600–750 °C. These phases do not have the same symmetry sites as anatase phase. As well, the formation of the pyrochlore phase at 750 °C induces a decrease of the transition at 610 nm ($^5D_0 \rightarrow {}^7F_2$ is forbidden).

The rutile lattice contains bigger octahedral sites than the anatase lattice, resulting in an easiest way for europium ions to enter in the rutile interstitial sites. On the other hand, the substitution of Ti^{4+} by Eu^{3+} is harder due to the higher density in the rutile phase. In the simple case of insertion, the C_{2h} symmetry will not decrease the luminescence emission considering there is no inversion center for the symmetry associated to europium in insertion sites. In opposite, Eu^{3+} ions substituting Ti^{4+} ions could tend to be segregated [[38]] and europium would be relocated to boundaries and lead to Eu–Eu quenching interactions or Eu_2O_3 formation, which will negatively affect luminescence by lowering the emission intensity, depending on the crystallographic structure of Eu_2O_3 formed [[39]]. Moreover, the presence of the pyrochlore structure $Eu_2Ti_2O_7$ [[1, 40]] is generally associated with a reduction of the $^5D_0 \rightarrow {}^7F_2$ and $^5D_0 \rightarrow {}^7F_0$ ED transitions intensity. The formation of the pyrochlore phase added two extra inequivalent positions for europium ions, one associated with a defect center and the other one center with an inversion symmetry. The shape of the $^5D_0 \rightarrow {}^7F_2$ transition is also different at 1 at. % of europium in Fig. 7. The main peak is divided in two peaks, a broad one at 613 nm and another one, sharper, at 618 nm. This surprising shape may be due the presence of Eu_2O_3 and rutile phases, increasing the amount of europium sites available and in fine, the amount of different electronic transitions.

All phases mentioned above are present for 1 and 5 at. % of europium and do not appear to affect negatively the luminescence intensity of the $^5D_0 \rightarrow {}^7F_2$ transition, contrary to the lifetime which increases until 700 °C to decrease after this temperature for 1 at. % and which is constantly decreasing on the thermal range studied for 5 at. % (Fig. 9). The apparition of other phases (for 1, 5 and 10 at. %) leads to a decrease of the lifetime by adding new crystallographic sites with new lifetime values for europium ions [[41]]. In contrast, the slow growth of crystallites in the sample doped at 5 at. % Eu^{3+} seems to be critical for the luminescence intensity since the intensity is quite the same than for 3 at.

% of Eu^{3+} (Fig. 7-c and Fig. 8). In opposite, the sample with the higher concentration (10 at. %) appears to be negatively affected by the apparition of the different phases. The combination of the pyrochlore formed in larger amounts (sufficient to be detected by XRD after treatment at 750 °C) due to a superior concentration of europium and a lower quantity of anatase compared to the rutile phase, decreases drastically the photoluminescence intensity at 700 °C and the lifetime, resulting in a lower intensity or lifetime than the sample fired at 600 °C. Nevertheless, it should be noted that the emission intensity remains in that case 250% or 225% higher than the one of the 3 at. % and 5 at. % respectively. The intensity loss being compensated by the larger amount of emitting center remaining in the 10 at. % sample. In the studied thermal range, the quantity of anatase is also extremely low compared to other samples, explaining the bigger impact of the other compounds in particular those affecting negatively the ED transitions (pyrochlore, europium oxide).

It is obvious that the Eu^{3+} doping increasingly shifts the stability of anatase phase toward elevated temperature, until a precise concentration (3 at. %). For higher concentrations (5 and 10 at. %) the system loses its stability with the apparition of other phases. Beside this effect, the luminescence absolute intensity of the $_5D^0 \rightarrow {}_7F$ [2] transition is significantly impacted when samples at 3 and 5 at. % of europium ions are compared. The one at 5 at. % should have an higher absolute intensity due to an higher amount of emitting center and surprisingly, sample at 3 at. % of europium has a superior intensity at 600 and 700 °C and a similar intensity at 750 °C compared to sample with 5 at. % of Eu^{3+} because of a bigger quantity of anatase phase (for 3 at. %) and the presence of secondary phases (for 5 at. %). Nevertheless, at any temperature, the sample at 10 at. % exhibits a quantity of anatase extremely low (2.2% at 600 °C and 3.2% at 750 °C) with the presence of rutile disordered, pyrochlore and europium oxide phases, compared to the sample at 3 at. % free from secondary-phases and with higher amount of anatase phase. Notwithstanding this major difference, sample at 10 at. % has 250% more luminescence absolute intensity. These results do not confirm the hypothesis stating that the sample with the bigger amount of anatase phase has the higher emission intensity. A possible explanation, if firstly considering sample at 5 and 10 at. %, could be that they do not have the same quantity of secondary-phases and the one at 5 at. % has the higher amount. Beside this fact, 10 at. % has more emitting centers available but mainly in amorphous environment. Eu^{3+} ions in this amorphous state may emits enough photons to have higher emission intensity compared to 5 at. % and even, higher emission intensity than 3 at. %. It is somewhat reminiscent of the fact that further work will be required to understand this difference of absolute emission intensity considering all the parameters.

4. Conclusions

Eu^{3+} doped TiO_2 powders synthesized by a sol gel-route were studied by X-ray diffraction, Raman spectroscopy and fluorescence spectroscopy to investigate the influence of Eu^{3+} concentration (in the range 1 at. %-10 at. %) and heat treatment temperature (in the range 600 °C–750 °C) on structural properties and fluorescence emission spectra. Main findings can be summarized as follow:

- Heat treated, TiO_2:Eu^{3+} appears to be a complex system characterized by the presence of various phases (anatase, rutile ordered/disordered, europium oxide Eu_2O_3, pyrochlore Eu_2TiO_7) depending on both the Eu^{3+} concentration and the heat treatment temperature;
- The simpler system is obtained with a concentration of 3 at. % of europium. It stabilizes a unique anatase phase with the highest level of crystallinity amongst the doped samples (from 60.6% to 71.6%) in the thermal range studied. Compared to the other concentrations investigated (1, 5 and 10 at. %), it shifts anatase-rutile transformation by at least 150 °C, avoids segregation of part of the europium content as Eu_2O_3, and inhibits formation of $Eu_2Ti_2O_7$ pyrochlore up to at least 750 °C. Nonetheless, the behavior after longer duration heat treatments (e.g. 1 h at least) should be studied to validate this hypothesis;
- Contrary to other samples, the one with 10 at. % of europium ions does not have a monotone increase of luminescence absolute intensity and 3 at. % is the only sample with an increase of lifetime decay on the thermal range studied;
- The advancement of the crystallization has a strong influence on luminescence properties because of the increase of the number of crystallographic sites available for europium ions increasing the amount of emitting centers and in fine, the luminescence absolute intensity;
- The formation of different phases (rutile ordered and disordered, anatase, europium oxide, pyrochlore) adds new crystallographic sites diversifying the possible position for europium ions and thus, the luminescence properties;
- Raman spectroscopy appears to be a powerful tool necessary to investigate variations of luminescence. XRD was able to detect 3 phases but with an overestimated temperature apparition of pyrochlore phase. Elsewhere, only the Raman spectroscopy was able to detect europium oxide and disordered rutile. Complementary to XRD, Raman spectroscopy seems essential to investigate the presence of phases in small amounts that could not be detected by XRD alone otherwise.

Novel conclusions

- TiO_2: Eu^{3+} doped at 3 at. % stabilizes the anatase phase until 750 °C and has the higher level of crystallinity as compared to 1, 5 and 10 at. %;
- In opposition to others samples (1, 3 and 5 at. %), 10 at. % of europium ions leads to a non-monotonic increase in the thermal range because of formed secondary phases (rutile, europium oxide and pyrochlore);
- Lifetime decay is more sensitive to the local ion environment, TiO_2: Eu^{3+} doped at 3 at. % is the only one to have a monotone increase of the lifetime.

Declaration of competing interest

The authors declare that they have no known competing financial interests or personal relationships that could have appeared to influence the work reported in this paper.

Acknowledgements

The authors acknowledge Marie Busquet for her support for dioxide titanium syntheses.

This research did not receive any specific grant from funding agencies in the public, commercial, or not-for-profit sectors.

References

[1] D. Avram, A.A. Patrascu, M.C. Istrate, B. Cojocaru, C. Tiseanu, Lanthanide doped TiO2: coexistence of discrete and continuous dopant distribution in anatase phase, J. Alloys Compd. 851 (2021), 111091.
[2] A. Boukerika, L. Guerbous, Annealing effects on structural and luminescence properties of red Eu3+-doped Y2O3 nanophosphors prepared by sol–gel method, J. Lumin. 145 (2014) 148–153.
[3] H. Zhang, Special Issue: rare earth luminescent materials, Light Sci. Appl. 11 (2022) 1–3.
[4] I. Bulus, Europium-doped boro-telluro-dolomite glasses for red laser applications_ Basic insight into spectroscopic traits, J.Non-Crystall Sol. 534 (2020), 119949.
[5] T. Kataoka, T. Hashimoto, S. Samitsu, Z. Liu, M. Tagaya, Coordination state control of citric acid molecules on europium(III) ion-doped hydroxyapatite nanoparticles for highly efficient photoluminescence toward biomedical applications, ACS Appl. Nano Mater. 5 (2022) 2305–2315.
[6] A.M. Lines, Z. Wang, S.B. Clark, S.A. Bryan, Electrochemistry and spectroelectrochemistry of luminescent europium complexes, Electroanalysis 28 (2016) 2109–2117.

[7] J.Y. Cho, K.-Y. Ko, Y.R. Do, Optical properties of sol–gel derived Y2O3:Eu3+ thin-film phosphors for display applications, Thin Solid Films 515 (2007) 3373–3379.
[8] S. Singh, Synthesis and spectroscopic investigations of trivalent europium-doped M2SiO5 (M = Y and Gd) nanophosphor for display applications, J. Mater. Sci. 31 (2020) 5165–5175.
[9] Y. Paz, Application of TiO2 photocatalysis for air treatment: patents' overview, Appl. Catal. B Environ. 99 (2010) 448–460.
[10] N. Rahimi, Review of functional titanium oxides. I: TiO2 and its modifications, Prog. Solid State Chem. 44 (2016) 86–105.
[11] Hengzhong Zhang, Jillian F. Banfield, Thermodynamic analysis of phase stability of nanocrystalline titania, J. Mater. Chem. 8 (1998) 2073–2076.
[12] E. Setiawati, K. Kawano, Stabilization of anatase phase in the rare earth; Eu and Sm ion doped nanoparticle TiO2, J. Alloys Compd. 451 (2008) 293–296.
[13] S. Hishita, I. M, K. Koumoto, H. Y, Inhibition mechanism of the anatase-rutile phase transformation by rare earth oxides, Ceram. Int. 9 (1983) 61–67.
[14] Z. AntiC, et al., Multisite luminescence of rare earth doped TiO2 anatase nanoparticles, Mater. Chem. Phys. 135 (2012) 1064–1069.
[15] M. Borlaf, Synthesis and photocatalytic activity of Eu3+-doped nanoparticulate TiO2 sols and thermal stability of the resulting xerogels, Mater. Chem. Phys. 144 (2014) 8–16.
[16] H.S. Lee, Yellow phosphors coated with TiO2 for the enhancement of photoluminescence and thermal stability, Appl. Surf. Sci. 257 (2011) 8355–8359.
[17] V. Serga, Study of phase composition, photocatalytic activity, and photoluminescence of TiO2 with Eu additive produced by the extraction-pyrolytic method, J. Mater. Res. Technol. 13 (2021) 2350–2360.
[18] R. Palomino-Merino, et al., Red shifts of the Eg(1) Raman mode of nanocrystalline TiO2:Er monoliths grown by sol–gel process, Opt. Mater. 46 (2015) 345–349.
[19] M.J. Pelletier, Quantitative analysis using Raman spectrometry, Appl. Spectrosc. 57 (2003) 20–42.
[20] T. Ohsaka, F. Izumi, Y. Fujiki, Raman spectrum of anatase, TiO2, J. Raman Spectrosc. 7 (1978) 321–324.
[21] Y. Hara, M. N, Raman spectra and the structure of rutile at high pressures, phys. stat. sol. 94 (1979) 317–322.
[22] J. Mrázek, Synthesis and crystallization mechanism of europium-titanate Eu2Ti2O7, J. Cryst. Growth 391 (2014) 25–32.
[23] K.A. I, X-ray diffraction and Raman studies on Ho: Eu2O3, J. Mol. Struct. 1128 (2017) 325–329.
[24] P. Melnikov, I.V. Arkhangelsky, V.A. Nascimento, A.F. Silva, L.Z. Zanoni, Thermal properties of europium nitrate hexahydrate, J. Therm. Anal. Calorim. 128 (2017) 1353–1358.
[25] K. Binnemans, Interpretation of europium(III) spectra, Coord. Chem. Rev. 295 (2015) 1–45.
[26] D.A.H. Hanaor, C.C. Sorrell, Review of the anatase to rutile phase transformation, J. Mater. Sci. 46 (2011) 855–874.
[27] M. Borlaf, Rare earth-doped TiO2 nanocrystalline thin films: preparation and thermal stability, J. Eur. Ceram. Soc. 34 (2014) 4457–4462.
[28] Y. Zhang, H. Zhang, Y. Xu, Y. Wang, Europium doped nanocrystalline titanium dioxide: preparation, phase transformation and photocatalytic properties, J. Mater. Chem. 13 (2003) 2261–2265.
[29] D. Komaraiah, et al., Effect of particle size and dopant concentration on the Raman and the photoluminescence spectra of TiO2:Eu3+ nanophosphor thin films, J. Lumin. 211 (2019) 320–333.
[30] C.-H. Hsu, et al., Air annealing effect on oxygen vacancy defects in Al-doped ZnO films grown by high-speed atmospheric atomic layer deposition, Molecules 25 (2020) 12.
[31] S. Mehraj, Annealing dependent oxygen vacancies in SnO2 nanoparticles: structural, electrical and their ferromagnetic behavior, Mater. Chem. Phys. 171 (2016) 109–118.
[32] U. Balachandran, N.G. E, Raman spectra of Titanium oxide, Solid State Chem. 42 (1982) 276–282.
[33] R.S. Ningthoujam, V. Sudarsan, R.K. Vatsa, R.M. Kadam, A. Gupta, Photoluminescence studies on Eu doped TiO2 nanoparticles, J. Alloys Compd. 486 (2009) 864–870.
[34] W.-N. Wang, W. Widiyastuti, T. Ogi, I.W. Lenggoro, K. Okuyama, Correlations between crystallite/particle size and photoluminescence properties of submicrometer phosphors, Chem. Mater. 19 (2007) 1723–1730.
[35] M. Chang, et al., Hydrothermal assisted sol-gel synthesis and multisite luminescent properties of anatase TiO2:Eu3+ nanorods, RSC Adv. 5 (2015) 59314–59319.
[36] J. Ovenstone, P.J. Titler, R. Withnall, J. Silver, Luminescence in europium-doped titania: Part II. High concentration range of Eu $^{3+}$, J. Mater. Res. 17 (2002) 2524–2531.
[37] X. Chen, W. Luo, Optical spectroscopy of rare earth ion-doped TiO $_2$ nanophosphors, J. Nanosci. Nanotechnol. 10 (2010) 1482–1494.
[38] S.M. Al-Shomar, Synthesis and characterization of Eu3+ doped TiO2 thin films deposited by spray pyrolysis technique for photocatalytic application, Mater. Res. Express 8 (2021) 16.
[39] W. Chen, et al., Structure, luminescence, and dynamics of Eu2O3 nanoparticles in MCM-4, Am. Chem. Soc. 106 (2002) 7034–7041.
[40] J. Mrázek, et al., Luminescence properties of nanocrystalline europium titanate Eu 2 Ti 2 O 7, J. Alloys Compd. 645 (2015) 57–63.
[41] S. Amiel, E. Copin, T. Sentenac, P. Lours, Y. Le Maoult, On the thermal sensitivity and resolution of a YSZ:Er3+/YSZ:Eu3+ fluorescent thermal history sensor, Sensor Actuator Phys. 272 (2018) 42–52.